

E-5-4

A Bias-Dependent Equivalent-Circuit Model of High Performance Evanescently Coupled Photodiode with Partially P-Doped Absorption Layer

 Y.-S. Wu¹, D.-M. Lin¹, F.-H. Huang¹, W. Y. Chiu¹, J.-W. Shi^{1*}, Y.-J. Chan¹
¹Department of Electrical Engineering, National Central University
 Taoyuan 320, TAIWAN, R.O.C.

 Tel: +886-3-4227151 ext. 34466 FAX:+886-3-4255830 Email: jwshi@ee.ncu.edu.tw

1. Introduction

Recently, the PDs with high available radio-frequency (RF) power under intense optical power excitation and high dc bias voltage attract lots of attention [1]. An accurate equivalent-circuit model for such high power photodiode (PD) under large-signal operation is thus very important in their applications, such as the resonating matching circuit design for fiber radio wireless communications systems, and trans-impedance amplifier circuit design [2]. In general, the frequency response of PD is affected by the bias voltage under high optical power excitation. Therefore, it is necessary to establish an equivalent model of PD under different optical power and dc bias voltages. In this paper, the bias-dependent and power dependent equivalent model was extracted to characterize the bandwidth degradation under low bias voltage and high photocurrent generation of an evanescently coupled PD (ECPD) with partially p-doped photo-absorption layer, which has demonstrated excellent current-bandwidth product (920mA-GHz) and responsivity (1.01 A/W) performance [3]. By incorporating the conventional model which includes the RC time limitation and transit time limitation, with the space charge screen effect in this small-signal radio frequency equivalent circuit [4], the simulated results fitted well to the measured frequency response of such device under varied bias voltage and different input power level in a broad frequency range 40 MHz to 40 GHz.

3. Equivalent Circuit

Fig. 1 presents the cross-sectional view of the evanescently coupled photodiode with 0.5 μ m partially p-doped photo-absorption layer and 150 μ m² active area. Such figure also shows what relation between the equivalent circuit components and the physics parameters of the ECPD, where R_c is the p-electrode contact resistance, R_j is the resistance of P⁺-InGaAs layer, and the parameter R_s is the resistance which indicate the summation of R_c and R_j ; C_j is the reverse bias junction capacitance, C_{dx} is the capacitance between the interconnected p-metal and n-electrode pad, and C_p is the p-electrode pad capacitance; L_s is the inductance of air-bridge from p-contact to p-electrode pad, L_G is the inductance induced by the n-electrode pad as an CPW ground pad, and the parameter L is the inductance which indicate the summation of L_G and L_s . The arranged equivalent circuit includes three bandwidth-limiting factor, which are RC delay time constant (f_{RC}), transit time (f_t), and the space charge screen effect (f_{csc}) respectively, and the total 3-dB bandwidth of the ECPD can be represented by Eq. (1).

$$\frac{1}{f_{3dB}^2} = \frac{1}{f_{RC}^2} + \frac{1}{f_t^2} + \frac{1}{f_{csc}^2} \quad (1)$$

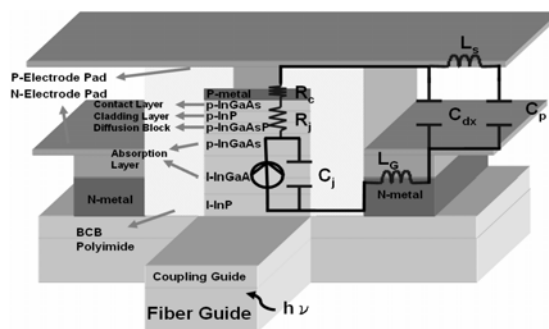


Fig. 1 The cross section of evanescently coupled photodiode with partially p-doped photo-absorption layer. The equivalent circuit elements are related to the ECPD parameters as shown.

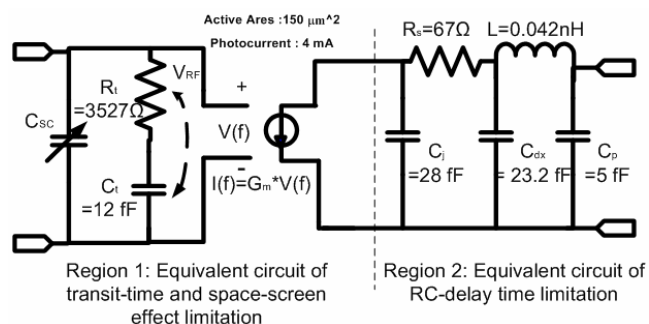


Fig. 2 Small-signal ration frequency model of ECPD that involves the parasitic elements, carrier transit-time effect, and the space-charge screen effect.

The limitation of RC delay time is described by the parameters that mentioned in Fig. 1. Regarding to the carrier transit time limitation, it is approximated by the $R_c C_t$ delay time as shown in region 1 of Fig. 2. The parameter C_{sc} is used to describe the degradation of frequency response that induced by the space charge screen effect. The ac photocurrent flow out to the external parasitic circuit was controlled by the ac voltage V_{RF} across the $R_c C_t$ and C_{sc} equivalent circuit. Therefore, the voltage controlled current source is represented as $g_m V_{RF}$, where g_m is a constant adjusted to the opto-microwave conversion quantum efficiency.

3. Measurement Results

A standard measurement process flow was performed to find out the exact values in this equivalent circuit. On the purpose of de-embedding the influence of passive RF pads and extract the parameters of active device precisely, the inductance L and the capacitance C_p , and C_{dx} , which are determined by the electrode

pad and the dielectric constant of passivation material respectively, were extracted through measuring the S-parameters of the electrode pad which was patterned on a dummy InP wafer with BCB passivation by using HP 8510C network analyzer. The same measurement setup was also performed on ECPD to measure the S_{22} parameter with different bias voltages and various input optical power. Through de-embedding the influence of RF pads off, the values of junction resistance R_s , and junction capacitance C_j were obtained. One can see from Fig. 3, where the trace of open circle means the measurement result and the solid line means the fitting trace. The model has a good curve fitting to the measured S_{22} parameter which was acquired by network analyzer under -3 V bias voltage. Finally, the frequency response was measured with different input power level and bias voltage by the heterodyne beating setup [2, 3] and through the use of the extracted RC-delay time model as discussed above, the parameters of R_t , C_t , and C_{sc} can be derived from fitting the traces of frequency responses.

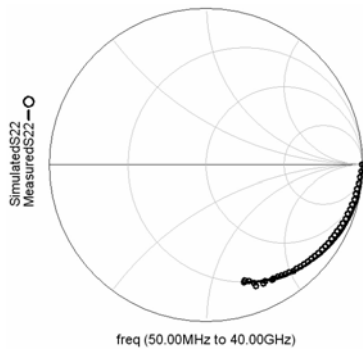


Fig. 3 Measured and calculated S_{22} versus frequency (from 40 MHz to 40 GHz) of ECPD on Smith chart.

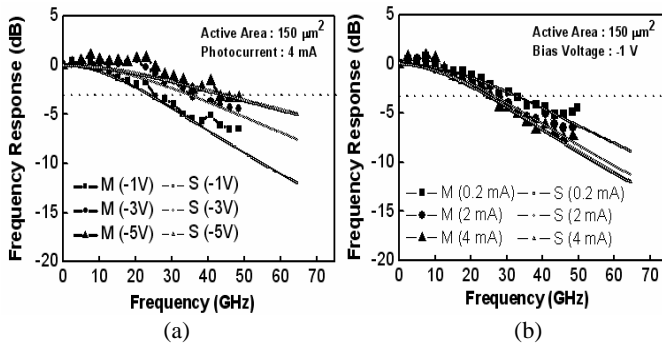


Fig. 4 The measured and calculated optical-microwave conversion parameters S_{21} of ECPD with $150 \mu\text{m}^2$ active area (a) under three different bias voltages (-1,-3, and -5V) and 4 mA photocurrent generation, and (b) under three different photocurrent generations (0.2, 2, and 4 mA) and -1 bias voltage.

Fig. 4(a) shows the frequency responses under different bias voltages (-1, -3, and -5) and fixed photocurrent (4mA), and Fig. 4(b) shows the frequency responses under different photocurrent (0.2, 2, and 4 mA) and fixed bias voltage (-1 V), which both are obtained by measuring the ECPD with $150 \mu\text{m}^2$ active areas through heterodyne beating setup, and the fitting traces of frequency response that simulated by the extracted equivalent circuit. It was found from this plot that we can get good fitting

traces by choosing the value of C_{sc} properly in this equivalent circuit. Fig. 5 shows the optimized fitting value of C_{sc} versus the bias voltage under various photocurrents. This result clearly shows that the device speed performance won't degrade under -5 V bias voltage due to the elimination of space-charge capacitance.

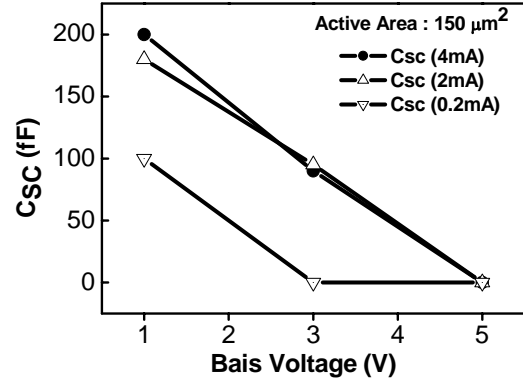


Fig. 5 The parameter C_{sc} which determined by fitting the frequency response versus the bias voltage under different power level.

4. Conclusions

In summary, an equivalent circuit model of high performance ECPD that includes the space charge screen effect, carrier transit time, and RC delay time is demonstrated to fit with the measured frequency response under different input power level and bias voltages. By concerning the relationship between the influence of bias voltage and photocurrent in the equivalent circuit-model of high power PD, such model is more convenient for systems and circuits integration especially under high RF power applications.

Acknowledgments

The authors are grateful to the financial support from the MOE Program for Promoting Academic Excellence of Universities. (Grant number 91-E-FA06-1-4), and the Ministry of Economic Affairs of Republic of China under the Program for Industrial Technology Development (91-EC-2-A-17-0285-029).

References

- [1] P. L. Liu and K. J. Williams, *IEEE Trans. Microwave Theory Tech.*, **47** (1999) 1297.
- [2] Hiroshi Ito and Satoshi Kodama, *IEEE J. Select. Topics Quantum Electron.*, **10** (2004) 709.
- [3] Y. S. Wu and J. W. Shi, *IEEE Photon. Technol. Lett.*, **17** (2005) 878.
- [4] Gang Wang, and Tsuneo Tokumitsu, *IEEE Trans. Microwave Theory Tech.*, **15** (2003) 1227.